The Engineering Society
For Advancing Mobility
Land Sea Air and Space®
INTERNATIONAL

400 COMMONWEALTH DRIVE, WARRENDALE, PA 15096-0001 U.S.A.

SAE Technical Paper Series

901988

Application of Favorable Aerodynamic Interference to Supersonic Airplane Design

Robert M. Kulfan
Boeing Commercial Airplanes Group
Seattle, WA.

Aerospace Technology Conference
and Exposition
Long Beach, California
October 1-4, 1990

901988

Application of Favorable Aerodynamic Interference to Supersonic Airplane Design

Robert M. Kulfan
Boeing Commercial
Airplanes Group
Seattle, WA.

ABSTRACT

There is a significant potential for improvements in cruise aerodynamic efficiency of supersonic aircraft through improved design methodology, friction drag reduction, innovative design and the use of favorable interference concepts. The use of favorable aerodynamics concepts such as supersonic biplanes, ring wing, parasol wing and caret wings for the design of a small supersonic aircraft is discussed. The parasol wing concept is shown to offer the greatest potential for improvements in lift/drag ratio relative to a conventional design. However, the best aerodynamic concept is very dependent on the design Mach number, and on the airplane component size relationships. Optimized nacelle installations for a High Speed Civil Transport, HSCT, have aerodynamic interference effects similar to the parasol wing concept.

INTRODUCTION

The purpose of this paper is to examine the potential benefits of using hypersonic favorable interference aerodynamic concepts in the design of supersonic aircraft.

Aircraft capable of extended range while cruising at supersonic Mach numbers are of interest for both commercial (1) * and military applications (2). Existing supersonic airplanes and current study configurations typically employ thin, highly swept wings and slender bodies that are integrated with the propulsion system and other components to produce aerodynamically efficient designs. Through careful design, these configurations can derive favorable aerodynamic interference effects associated with mutual interactions of the flow fields created by the airplane components. These interactions can result in direct drag reduction, or in additional lift production. Body area ruling (3) and wing mounted engine installations (4) are well-known examples.

In this paper it is shown that there is a potential for significant increases in cruise lift/drag ratios over conventional supersonic designs. These improvements can have a significant impact on the viability of a High Speed Civil Transport.

One of the means to achieve improvements in aerodynamic efficiency is by enhancing favorable aerodynamic interference effects. A study of utilizing hypersonic favorable interference for supersonic aircraft (5,6) is reviewed. The parasol wing concept was identified as the most promising concept. This concept is applied to the design of a small supersonic aircraft.

It is shown that achieving favorable nacelle interference on a large supersonic configuration incorporates many of the aerodynamic features of the parasol wing concept.

TYPES OF AIRCRAFT

Classes of airplanes can be defined according to the types of flow associated with the airplane (7,8). Four types of aircraft are identified in Figure 1.

The classical and swept wing aircraft are quite similar. In fact, the swept wing aircraft is an extension to higher speeds of the classical aircraft concept. The flow over these wings is nearly two-dimensional in streamwise planes. The wings have sharp trailing edges, so that flow separation is confined and fixed to the trailing-edge area.

* Numbers in parenthese designate references at end of paper

It is possible to control this type of flow, and the associated forces and moments, to allow a sufficient range of practical flight conditions. The flow of these configurations is essentially subsonic with regions of transonic flow. Means for providing volume, lift, thrust, and control are typically separate from each other.

The flow over slender wings is effectively subsonic except, perhaps for localized areas near the wing trailing edge. The flow over these wings is attached for a rather limited angle of attack regime. A series of design criteria for achieving attached flow at supersonic speeds are discussed in Reference 9.

The most obvious aerodynamic characteristic of slender wings is the formation of rather stable leading-edge vortices at increased angle of attack, Figure 2. The angle of attack at which the flow separation and leading-edge vortices start, depends on the airfoil leading-edge radius, and wing camber and twist (10). The flow is attached on the wing behind the vortices, up to high incidence angles. When the leading-edge vortices develop, the drag due to lift increases because of loss of leading-edge suction (10). The lift and pitching moment continue to increase. The components of the airplane that provide lift, volume, and thrust again tend to be separate. However, the components are carefully tailored to maximize aerodynamic efficiency through mild favorable interference effects (3).

The final class of aircraft, and the one of particular interest for this study, is the wave producer family. This family has been studied in conjunction with hypersonic configurations. The wave producer family differs from the previously mentioned types of aircraft in the following principal areas:

- Flow over the configuration is fundamentally supersonic at cruise. Shock waves and expansion waves in the stream are a predominant feature of the flow, and cannot be avoided. The shock waves are used to produce compression lift. The shock waves and expansion waves can interact to produce drag reductions.
- At lower speed, the flow changes to a subsonic type of flow similar to the slender wing. The change in flow is gradual and controllable.

Aircraft of the wave producer family tend to be highly integrated. In some concepts, the volume, lift, and thrust producing components are aerodynamically indistinguishable. Only the slender wings and wave producing concepts are acceptable for high supersonic cruise flight.

SUPERSONIC DRAG

The drag of a conventional airplane at supersonic speeds consists of four major drag items:

- Skin friction drag, CDF
- Vortex drag, as in subsonic flow, CDV
- Wave drag due to volume, CDW
- Wave drag due to lift CDWL

A convenient way to characterize the aerodynamics and geometry of the various types of aircraft, as shown in Figure 3, is by the slenderness ratio, s/l. This is the ratio of the wing semi-span to overall airplane length. Figure 3 shows the effect of the aircraft slenderness ratio on these drag components. As the Mach number is increased, the optimum aircraft becomes more slender. This is to compensate for increasing wave drag due to lift. Typical maximum lift/drag ratios (L/D)max for slender wing configurations are shown in Figure 4.

POTENTIAL FOR L/D IMPROVEMENTS

Let us examine the potential for improvements in aerodynamic efficiency, (L/D)max, for current conventional supersonic design concepts. It is convenient to express the supersonic drag as the sum of two major components.

The first component is the zero lift drag (CDo) which does not vary with angle of attack. This includes friction drag and volume wave drag. The second component approximates the lift dependent drag using an "equivalent" drag-due-to-lift factor (KE). The lift dependent drags

includes the vortex drag and the wave drag due to lift. The maximum lift/drag ratio can be related to CDo and KE as shown in Figure 5.

Boundaries for zero lift drag, CDo, and for drag-due-to lift factor KE are shown in Figure 6 for a typical HSCT design.

The minimum zero lift drag for fully turbulent slender aircraft is equal to flat plate turbulent skin friction drag plus the wave drag of a Sears Haack body having the same volume and overall length as the complete aircraft. The maximum zero lift drag of an acceptable configuration shown in this figure includes the flat plate skin friction drag plus the wave drags of the isolated components. The minimum level for drag due to lift corresponds to the drag of an optimum isolated cambered wing design. An appropriate maximum level for drag due to lift is equivalent to the drag of a flat wing without leading edge suction. These boundaries for CDo and KE define the regions of acceptable conventional supersonic aircraft designs.

Figure 7 shows a typical carefully tailored conventional supersonic aircraft. The aerodynamic efficiency of this configuration developed using current aerodynamic design ideas and optimization methods is shown in the "acceptable design" region in Figure 8. These design methods which were developed in support of the US SST program are at least twenty years old.
It is evident that there is a potential for a significant improvement in aerodynamic efficiency. This will require development of improved design optimization tools and better detailed design integration procedures that use the emerging advanced CFD methods.

The effect of improvements in cruise drag on an HSCT designed for a specific mission is summarized in Figure 8. A 1% drag reduction will reduce maximum takeoff gross weight, MTOW, by 10,000 lbs and also results in a fuel saving of 6,000 lbs. This is equivalent to an operating empty weight, OEW, reduction of 3,000 lbs. It is obvious that achieving even a fraction of the potential L/D improvement indicated in Figure 8 would have a major impact on the viability of an HSCT.

Figure 9 shows that additional improvements in L/D can be achieved by expansion of these boundaries through friction drag reduction (11) and using innovative aerodynamic concepts such as the oblique wing concept (11, 12). Enhancing favorable aerodynamic interference effects offers additional possibilities for increases in supersonic aerodynamic efficiency. Considerable development of favorable aerodynamic interference technology took place in studies of maneuverable orbital entry vehicles and hypersonic vehicles. Application of these favorable aerodynamic interference concepts to supersonic aircraft has not been explored in depth.

A study (5, 6) was made to evaluate potential aerodynamic benefits of using these hypersonic concepts for supersonic aircraft. The aerodynamic design results of that study are summarized in this paper.

AERODYNAMIC CONCEPT SELECTIONS

The identification of candidate favorable aerodynamic interference concepts that were considered, was initiated by a literature survey of technical references. The literature search revealed a number of potentially applicable interference concepts, shown in Figure 10. Qualitative assessments were made to determine which of these concepts were most suitable for application to meet the mission and design objectives.

The caret wing, Nonweiler wing, supersonic biplane, and parasol wing concepts were then identified as the potentially most promising concepts. The study effort was then directed at obtaining a fundamental understanding of the desirable aerodynamic features of the selected concepts, and to better define the potential aerodynamic efficiency of configurations incorporating these concepts. Aerodynamics of the various concepts are discussed in the sections that follow.

A principal design Mach number of 3.0 was selected . This selection eased the design integration tasks of incorporating the favorable aerodynamic interference concepts. This

aerodynamic design task becomes more difficult at lower supersonic Mach numbers, because of the greater areas of the flow field affected by shock waves and expansion waves produced by the aircraft components. The configurations considered in the study were representative of a small supersonic cruise military type aircraft.

SUPERSONIC BIPLANES

The Busemann supersonic biplane offers the potential of significant reduction in wing thickness drag (13, 14, 15, 16). The drag reduction, as shown in Figure 11, can be obtained by mutual thickness interference between two wing panels, and also by interference between the lifting pressures on one wing acting on the thickness on an adjacent wing panel. The Busemann biplane type of interference is commonly called wave cancellation, since the shock waves produced by one surface are cancelled by an expansion pressure field produced on an adjacent surface.

Adjacent reflection surfaces are necessary to achieve the drag reduction. The reflection surface increases the friction drag. The drag due to lift is typically higher than that of the isolated individual surfaces as shown in Figure 12.

The wing thickness wave drag reductions must exceed increases in friction drag, and drag due to lift, to show any net cruise drag benefit. The net aerodynamic benefits of a supersonic biplane were considered typically small, and were not investigated further.

CARET AND NONWEILER WINGS

Previous hypersonic studies (9, 17 through 21) have indicated that the caret wing and Nonweiler wing concepts offer higher aerodynamic efficiency potential at very high supersonic Mach numbers than do conventional slender wing configurations. The aerodynamic features of the caret wing and Nonweiler wing concepts are shown in Figure 13. The caret wing is designed to produce the same flow field as an equivalent two-dimensional wedge having its top lined up with the free stream. In an inviscid flow, the wedge shock wave is attached to the leading edge, and is a plane surface below the wedge.

The upper surface of the caret wing is aligned with the free stream. The wing leading edge at the supersonic design condition lies on the equivalent wedge planar shock wave. The caret wing lower surface is formed by streamlines in the flow behind the shock wave that passes through the wing leading intersection. This results in a three-dimensional wing configuration with an open base, and has the undisturbed free stream pressure over its top surface. The pressure on the lower surface is uniform, and equal to the pressure behind the shock in two-dimensional wedge flow.

The Nonweiler wing is formed by addition of an interference wing to a caret wing. The interference wing increases lift without increasing the slope of the main wing.

Exact shock wave relations were used to calculate the effects of Mach number, wedge angle, and planform slenderness ratios, s/l, on the design lift/drag ratios of caret wings. Results are shown in Figure 15.

The optimum wedge angle of the caret wing is approximately 4 deg at Mach 3.0, and increases slightly with higher design Mach numbers. Wing slenderness ratios in the order of 0.3 to 0.5 result in lift/drag ratios near maximum. Hence, the optimum caret wing has a larger wing span than the optimum slender wings shown in Figure 4.

The anhedral angle of the caret wing depends on the wedge angle, slenderness ratio, and design Mach number of the caret wing as shown in Figure 14. The large anhedral at lower Mach numbers probably restricts the usefulness of the caret wing to higher supersonic Mach numbers.

FLAT-TOP WING/BODY CONFIGURATION

An alternative form of a wave rider concept is the flat-top wing/body arrangement (22 through 27). The body area growth under the wing produces a bow shock, followed by a compression pressure field. The wing leading edge coincides with the bow shock at the design Mach number. The body pressures, as shown in

Figure 16, fall upon the wing lower surface to produce an interference lift increment.

The body wave drag of this configuration, however, is greater than the body wave drag of an equal area symmetric wing/body configuration. The wing lower surface pressures, when the wing is at an angle of attack, push on the forebody, producing an unfavorable wing-on-body interference. The unfavorable wing-on-body interference and the increase in body wave drag tend to cancel the favorable lift interference effects.

The potential aerodynamic benefits of a flat-top wing/body concept over a symmetric wing/body arrangement are, at best, small.

RING WINGS AND PARASOL WINGS

The ring-wing configuration (Figure 10) is a three-dimensional application of the Busemann biplane wave cancellation concept. The ring wing is designed to reflect forebody compression pressures back, to push on the aft end of the body. This effect can result in zero body wave drag.

The half-ring wing concept retains part of the body wave drag cancellation, but produces an interference lift associated with the forebody pressures glancing off the wing lower surface. This effect produces a more efficient lifting system.

The parasol wing concept is a further adaptation of the half-ring wing concept designed to enhance the overall aerodynamic efficiency of the configuration.

Previous investigations (26, 28 through 42) have shown that the parasol wing/body arrangement can combine wave-cancellation and interference lift effects into an aerodynamically efficient design. The body in a parasol wing arrangement is position below the wing, so that, at supersonic speeds, the bow shock and forebody pressure field impact on the wing lower surface. The body wave cancellation effect is produced by the body pressures glancing off the wing surface, and back onto the aft end of the body. This effect produces a thrusting force. The body pressures reflecting off the wing also produce a favorable interference lift force. The wing lower surface lifting pressures push on the aft end of the body to produce a favorable thrust force. The aerodynamic features of the parasol wing are shown in Figure 17.

Parametric studies were made to investigate body wave drag cancellation, and interference lift generation for a body located below a wing. The objective of these investigations was to scope aerodynamic benefits of configurations employing the parasol wing concept. The studies focused on identifying the importance of body spacing, wing dihedral, and parasol curvature effects for enhancing the body wave drag cancellation and interference lift production, and to provide design guidelines for developing a parasol wing configuration.

Results of these studies which are summarized in part below are presented in more detail in Reference 10.

The amount of body wave drag cancellation is affected by the distance between the body and parasol reflection surface and can be enhanced by the anhedral or lateral curvature of the planform. The effects of flat wing reflection, 45% dihedral wing, half-shroud wing, and full-shroud wing on body wave drag are shown in Figure 18. The optimum half-shroud arrangement reduced the body wave drag by nearly 50%.

Additional wave drag analyses were made of the simple rectangular half-shrouded wing arrangement. Shroud geometries having different ratios of shroud width, Sw, to shroud height, Sh, were investigated. For each arrangement, the shroud height was varied to determine the minimum drag arrangement. The optimum shroud geometries for the rectangular shroud are shown in Figure 19. These results indicate that for a design Mach number of 3.0, a low-drag shroud should have a semispan of 1.4 body diameters, and be located 1.2 diameters above the body centerline.

The body pressures acting on the reflection surfaces of the flat wing, dihedral wing, or half-shrouded wing also produce an interference lift. The amount of interference lift depends on the portion of the body pressures by

the wing surface and on the lateral curvature or anhedral of the wing. As shown in Figure 20, these curvature effects can increase the interference lift by more than 50% relative to a flat wing.

Theoretical investigations were made to compare the aerodynamic characteristics of a parasol, designed to capture interference lift from a typical Mach 3.0 nacelle (open nose body), with a parasol designed to capture interference lift from a fuselage (closed nose body). The calculated wave drag for the nacelle in the presence of a parasol is shown in Figure 21. These results indicate that the nacelle centerline should be located approximately 0.7 to 0.8 of the maximum body diameter below the wing, to achieve maximum wave drag cancellation effects. It also appears that the wave drag of the nacelles can be reduced by 10% to 40%, depending on the parasol lateral curvature. Results of a similar study for the fuselage were shown in Figure 19. The fuselage must be located approximately 1.4 body diameters below the wing to achieve optimum wave cancellation. This distance is much greater than that required for the nacelle parasol.

The forecowl angle of a nacelle offers the capability to increase interference lift. The forecowl angle should be selected to optimize the trade between increased interference lift, and the adverse effects of increased nacelle wave drag and nacelle weight.

The theoretical pressure distributions calculated on a planar wing above a pointed nose body representing a fuselage, and above an open nose body representing an engine nacelle, are shown in Figure 22 and Figure 23. These pressure distributions reveal a negative pressure region, which diminishes the lift produced by the positive pressures. If this region is eliminated, appreciably higher interference lifts can be obtained .

Theoretical predictions of interference lift for planforms tailored to capture only the positive pressures are shown in Figure 24. Interference lift is seen to increase dramatically over the slender body theory maximum value. To minimize the capture area and maximize the interference lift, the wing planform should be designed so that the leading edge matches the body bow shock in the plane of the wing, and the trailing edge cuts off any negative interference pressures on the wing.

PARASOL WING CONFIGURATION DEVELOPMENT

Wing parasol geometries were calculated for a typical Mach 3.0 nacelle, and for a fuselage. The results are shown in Figure 25 and Figure 26. The body parasol is quite far from the body and would, therefore, require a pair of rather large struts. The nacelles can be supported by a single short strut, thus saving both weight and drag. The wing span for the body parasol is much larger than the span for the nacelle parasol. However, a configuration design incorporating a nacelle parasol on each side of the fuselage would have approximately the same span as the fuselage parasol.

The double-parasol wing configuration, shown conceptually in Figure 26, was selected for the final favorable interference concept.

The double-parasol wing planform was derived using design guidelines which were developed from the parametric studies (6). The nacelles are located 0.8 body diameters below the wing chord plane. The wing planform was designed to capture the nacelle interference pressures. The projected hyperbolic wing planform shape is designed for the maximum amount of nacelle interference lift per unit wing area. The planform curvature in the front view was designed to enhance the interference lift generation. The planform has a parabolic curvature between the nacelle and the body, and an additional parabolic section near the wing tip. The nacelle is at the focus of each parabolic section. The flat midwing section provides additional wing span and greater lift capture area.

The nacelles are tilted down, relative to the wing, to better align the inlets with the free stream, and to increase the interference lift. The wing leading edge inboard of the nacelle increases the wing root chord, and blends into the leading edge determined from the bow shock location calculations. The final parasol wing

planform and the Mach 3.0 design interference lift areas are shown in Figure 27.

The optimum wing camber and twist distribution for this configuration was modified to minimize the unfavorable nacelle/wing interference drag. The body has been area ruled to optimize the body/nacelle and body/wing interference effects.

The double-parasol wing favorable interference configuration, shown in Figures 28 and 30, is representative of a Mach 3.0 small supersonic military aircraft.

Calculated maximum lift/drag ratios for the double-parasol wing configuration are compared in Figure 31 relative to the corresponding values for a conventional type aircraft designed (5) for the same mission requirements. The reference conventional aircraft shown in Figure 29 had a flat wing design. The effect of incorporating an optimized wing camber and twist is also shown for the conventional design.

The double-parasol wing configuration at the Mach 3.0 design condition offers a potential improvement in the lift/drag ratio of approximately 25% relative to the reference flat wing configuration. Optimizing the nacelle area growth of the parasol wing configuration increases the potential lift/drag improvement to 37%. This increase is approximately 20% greater than the lift/drag ratio of the conventional aircraft with an optimized wing design. Additional theoretical and coordinated experimental studies will be necessary to fully identify the potential aerodynamic benefits of the configuration concept.

NACELLE FAVORABLE INTERFERENCE ON A HIGH SPEED CIVIL TRANSPORT

The double-parasol configuration was developed for a small supersonic fighter in which the engine is large compared to the required wing area. The engines on a High Speed Civil Transport, HSCT, are small compared to the wing area. The wing, however, can capture and derive favorable interference from the nacelle compression field much in the same manner as in the double-parasol configuration.

The installed drag for nacelles mounted in the wing of an HSCT consists of the skin friction drag, wave drag and effect of the interference lift on the configuration lift dependent drag (43). The nacelle installed wave drag as shown in Figure 32 consists of the isolated nacelle drag plus mutual interference between the wing thickness and the nacelles, plus mutual nacelle interference effects. Locating the nacelles aft on the wing so that the nacelle pressures "push" on the wing and the expansion pressures of the wing "suck" on the nacelles tends to cancel the isolated nacelle drag. Favorable interference can also be derived from the nacelles if the nacelles are separated or staggered so that the compression pressures form the adjacent nacelles or the nacelle pressure glancing off the wing push on the nacelles boattail. However, configuration design constraints typically do not allow the optimum nacelle spacing to be used.

The lift interference effects are also shown in Figure 32. Locating the nacelles aft and under the wing produces lift from the captured nacelle pressure field. For a specified total lift, the incremental nacelle lift allows the wing to fly at a lower incidence angle. This reduces the drag due to lift of the wing. This favorable effect is somewhat diminished by the unfavorable effects of the nacelle pressure field pushing in the wing camber and the lifting pressure field pushing in the nacelle fan cowl. Local wing tailoring can some reduce these two adverse effects.

As shown in Figure 33, the nacelle installed drag for a favorable aft nacelle location can be equal to, or less than the isolated nacelle friction drag. The installed drag for nacelles moved forward under the wing is shown in Figure 34. This shows that adverse interference effects can actually result in an installed drag that is significantly greater than the isolated drag.

Figure 35 shows the installed nacelle drag at a cruise for an optimized HSCT configuration. Again the nacelle installed drag is less than the isolated skin friction drag. The drag reduction at a lift coefficient of CL = 0.1 relative to the isolated nacelle drag is approximately six drag

counts (CD = .0006) using the sensitivities shown in Figure 9, this results in a reduction of maximum takeoff weight of approximately 60,000 lb.

Further reduction in the nacelle installed drag, that would be possible if the enhanced lift interference and wave drag cancellation of the double-parasol configuration could be achieved, are shown in Figure 36.

CONCLUSIONS

- There is a large potential for (L/D)max improvements through the use of advanced design methodology for conventional type HSCT aircraft. There is further potential for significant increases in (L/D)max through the use of non-planar interference effects, viscous drag reduction and unconventional aircraft concepts.

- The benefits and optimum configuration features for achieving favorable non-planar interference effects are dependent on the relative size of the aircraft components and on the design Mach number. The interference concepts considered in this study become more difficult to integrate into a viable aircraft configuration as the design Mach number is reduced.

- The parasol wing concept was identified as offering the greatest potential aerodynamic benefits, relative to the other concepts considered (wave riders, supersonic biplanes, flat-top wing bodies) for a small supersonic aircraft.

- The aerodynamic characteristics of a low drag nacelle installation on an HSCT are similar to the aerodynamics of the parasol wing concept.

REFERENCES

1. Proceedings of the SCAR Conference NASA CP-001, Vol. I and Vol. II, NASA-Langley Research Center, November 1976.

2. Design Conference Proceedings: "Technology for Supersonic Cruise Military Aircraft", Vol. I and Vol. II, USAF Academy, Colorado Springs, Colorado, February 1976.

3. Kane, E. J., and Middleton, W. D., " Considerations of Aerodynamic Interference in Supersonic Airplane Design", Paper No. 3, AGARD Conference Proceedings No. 71, September 1970.

4. Sigalla, A., and Hallstaff, T. H.: "Aerodynamics of Powerplant Installations on Supersonic Aircraft", Journal of Aircraft, pp 273--.277, July--August 1967.

5. Kulfan, R. M., Friebel, G. O., Lord B. J., and Yoshihara, H. : "Application of Supersonic Favorable Aerodynamic;Interference to Fighter Type Aircraft". AFFDL-TR-78-33, April 1978.

6. Kulfan, R. M. : "Application of Hypersonic Favorable Aerodynamic Interference Concepts To Supersonic Aircraft", AIAA Paper 78-1458, August 1978.

7. Kuchemann, D. : "Aircraft Shapes and Their Aerodynamics for Flight at Supersonic Speeds," In: Advances in Aeronautical Sciences, Zurich, 1960, Vol II, pp 221--252, Pergomon Press, Oxford, 1962.

8. Kuchemann, D. : "Hypersonic Aircraft and Their Aerodynamic Problems,: In: Progress in Aeronautical Sciences, Vol 6, 1965.

9. Kulfan, R. M., and Sigalla, A. : "Real Flow Limitations in Supersonic Airplane Design, AIAA Paper 78-147, January 1978, Journal of Aircraft Vol 16, Number 10, October 1978, pp 645-658.

10. Kulfan, R. M. : "Wing Geometry Effects on the Development of Leading Edge Vortices", AIAA Paper 79-1675, August 1979.

11. Bushnell, D. : "Supersonic Aircraft Drag Reduction", AIAA Paper 90-1596, June 1990.

12. Jones, R. T. : "Reduction of Wave Drag by Antisymmetric Arrangement of Wings and Bodies", AIAA Journal, Vol 10, No 2, February 1972, pp 171-176.

13. Beane, B. J., "Notes on the Variation of Drag with Mach Number of a Busemann Biplane", Douglas Aircraft Company Rep., S. M. 18737.

14. Graham, E. W., et al. : "A Theoretical Investigation of the Drag of Generalized Aircraft Configurations in Supersonic Flow, NASA TM 1421, January 1957.

15 . Graham, M. E. : "Application of Drag-Reduction Methods to Supersonic Biplanes, Douglas Aircraft Company Report No. SM-19258, September 1955.

16. Licher, R. M. : "Optimum Two-Dimensional Multiplanes in Supersonic Flow, Douglas Aircraft Rep. S. M. 18688, 1955.

17. Flower, J. W. : "Configurations for Higher Supersonic Speeds Derived from Simple Shock-Waves and Expansions," Journal of R. A. S., May 1963.

18. Nonweiler, T. : "Delta Wings of Shapes Amenable to Exact Shock Wave Theory", Journal of R. A. S., Vol 67, pp 39--40, January 1963.

19. Peckham, D. H. : "On Three-Dimensional Bodies of Delta Planform Which Can Support Plane Attached Shock Waves, A. R. C. C. P. No 640, March 1962.

20. Squire, W. C. : "Pressure Distributions and Flow Patterns at M = 4.0 on Some Delta Wings ", ARC R & M No 3373, 1964.

21. Squire, L. C. : "Calculated Pressure Distributions and Shock Shapes on Thick Conical Wings at High Supersonic Speeds", Aeronautical Quarterly, Vol XVIII, Part 2, pp 185--206, May 1967.

22. Goldsmith, E. L., and Cook, P. H. : "Some Mutual Interference Effects Between a 5.7 Cone and a Sonic L. E. Delta Wing at M = 2.49", R. A. E. Tech. Note No Aero 2936, 1964.

23. Eggers, A. J., Jr., and Syvertson, C. A. : " Aircraft Configurations Developing High Lift Drag Ratios at High Supersonic Speeds", NACA RM A 55L05, 1956.

24. Eggers, A. J., Jr. : "Some Considerations of Aircraft Configurations Suitable for Long-Range Hypersonic Flight", In: Hypersonic Flow (Editors A. R. Collar and J. Tinkler) Butterworth, London.

25. Goldsmith, E. L., and Cook P. H. : "Half Body and Wing Combinations in Supersonic Flow": "A Review of Some Principles and Possibilities", R. A. E., Tech. Report 65040, 1965.

26. Boyd, J. A. : "Optimal Utilization of Supersonic Favorable Interference to Obtain High Lift-Drag Ratios, AIAA Paper 65-752, November 1965.

27. Brown, C. E., and McLean, F. E. : "The Problem of Obtaining High Lift-Drag Ratios at Supersonic Speeds," J. A. S., pp 298--302, May 1959.

28. Sigalla, A. : "The Optimization for Minimum Wave Drag of a Fuselage Located Under a Wing", Boeing Airplane Company Report D6-5189, December 1959.

29. Chen, C. F., and Clarke, J. H. : "A Study of Configurations Composed of a Body Under a Lifting Wing in Supersonic Flow, Division of Engineering, Brown University, Air Force Office of Scientific Research TN 59-1276, 1960.

30. Chen, C. F., and Clarke, J. H. : "Body Under Lifting Wing", J. A. S., vol 28, No 7, pp 547--562, July 1961.

31. Clarke, J. H. : "The Forces on Wing-Fuselage Combinations in Supersonic Flow, Boeing Document D 1-82-0018, August 1959.

32. Cook, P. H. : "Further Experimental Results on the Mutual Interference Between Separated Wings and Bodies at M = 2.49", R. A. E. Tech. Report No. 66228, July 1966.

33. Gapcynski, J. P., and Carlson, H.: "A Pressure-Distribution Investigation of the Aerodynamic Characteristics of a Body of Revolution in the Vicinity of a Reflection Plane at Mach Numbers of 1.41 and 2.01, NACA RM-L54J29, October 1954.

34. Graham, E. W., and Licher, R. M. : "The Calculation of Interference Drag Between Wing Lift and Fuselage Thickness at Supersonic Speeds, Douglas Aircraft Report No SM-23446, February 1959.

35. Jones, R. T.: "Minimum Wave Drag for Arbitrary Arrangements of Wings and Bodies", NACA TN 1335, 1957.

36. Ferri, A. Clarke, J. H., and Ting, L. : "Favorable Interference in Lifting Systems in Supersonic Flow", J. A. S., vol. 24, No 11, pp 791--804, November 1957.

37. Morris, O. A., and Lamb, M. : "Aerodynamic Characteristics in Pitch of a Modified Half-Ring-Wing-Body Combination and a Swept Wing-Body Combination at Mach 2.16 to 3.70, NASA TM X-1551, April 1968.

38. Morris, O. A., and Mack, R. J.: "Aerodynamic Characteristics of a Parasol-Wing Body Combination Utilizing Favorable Lift Interference at Mach Numbers from 3.00 to 4.43, NASA TN D-4855, October 1968.

39. Mysliwetz, F.: "Supersonic Interference of a Body Under a Wing", Boeing Document D6-5207, July 1960.

40. Mysliwetz, F.: " Supersonic Interference Lift of a Body-Wing Combination, AIAA Journal, Vol 1 pp 1432--1434, June 1963.

41. Woodward, F. A.: "Pressures and Forces on Wings and Bodies in Close Proximity at Supersonic Speeds", Boeing Document D6-8927, April 1962.

42. Barger, R. L.: "Procedures for Designing Supersonic Bodies of Revolution from Prescribed Pressure Distributions, Paper No. 4, in "Analytic Methods in Aircraft Aerodynamics NASA SP-228, October 1969.

43. Kulfan, R. M. ; Sigalla, A. : "Airframe-Propulsion System Aerodynamic Interference Predictions at High Transonic Mach Numbers Including Off-Design Engine Airflow Effects", Paper 35, Agard Conference Proceeding No 301, "Aerodynamics of Power Plant Installations", May 1981.

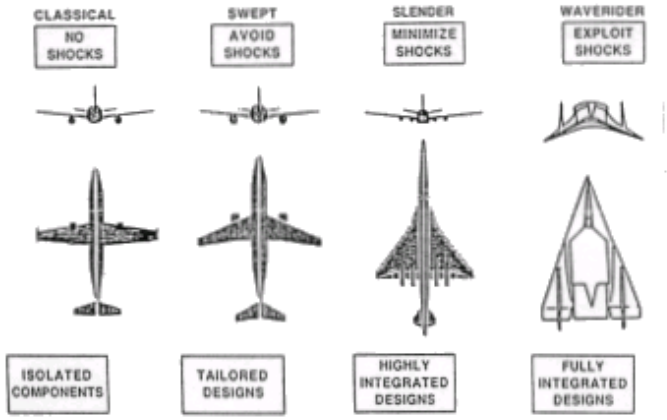

Figure 1 Types of Aircraft

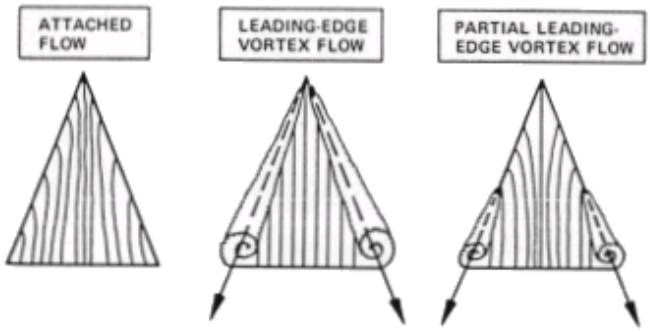

Figure 2 Types of Flow on Slender Wings

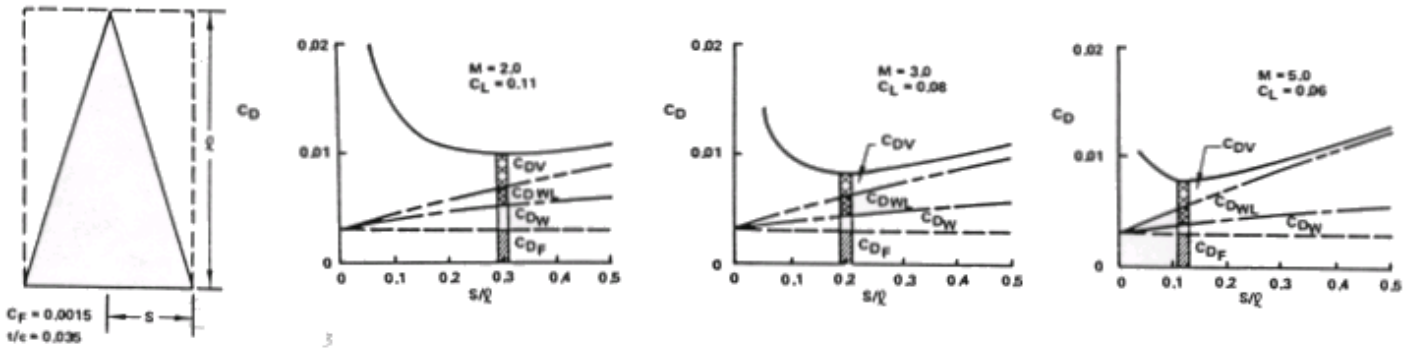

Figure 3 Slender Wing Supersonic Drag Components

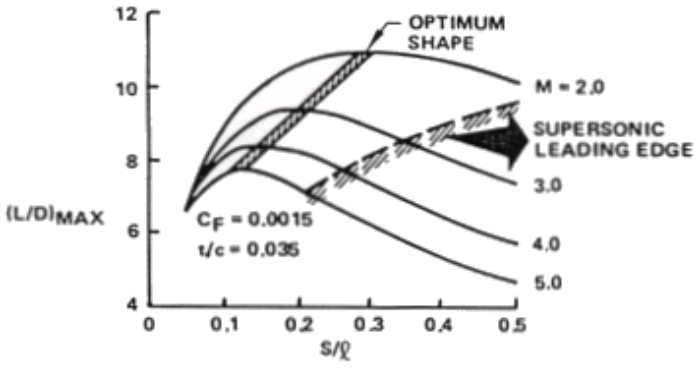

Figure 4 Slender Wing Maximum Lift/Drag Ratios

$$CD = CDO + KE * CL^2$$

$$(L/D)max = \frac{0.5}{\sqrt{KE * CDO}}$$

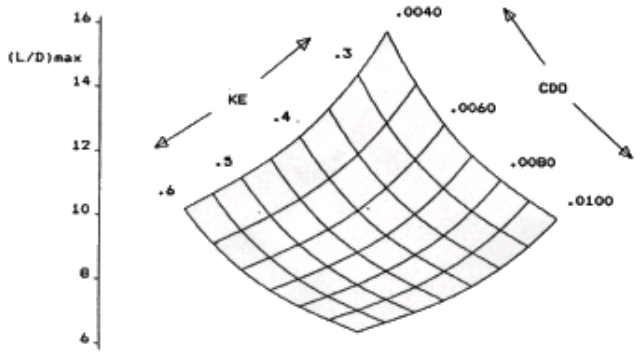

Figure 5 Effect of CDO and KE on (L/D)max

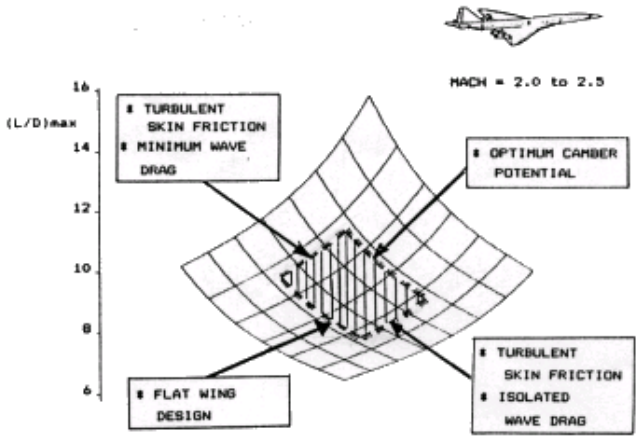

Figure 6 Drag Boundaries for Typical HSCT Configuration

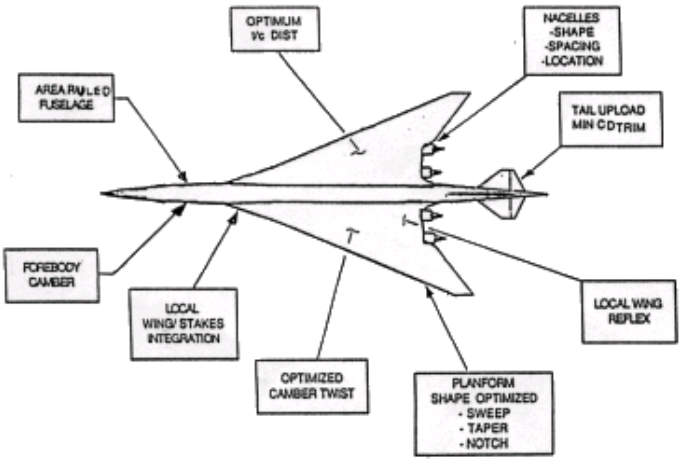

Figure 7 HSCT Aerodynamic Design Features

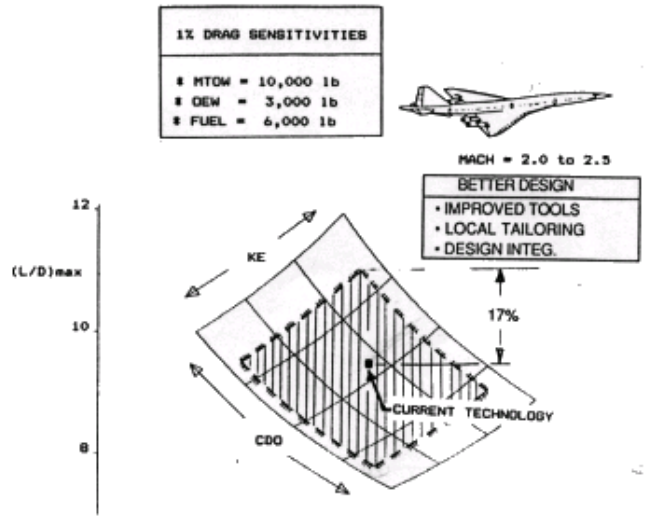

Figure 8 Potential (L/D)max Improvement - Better Designs

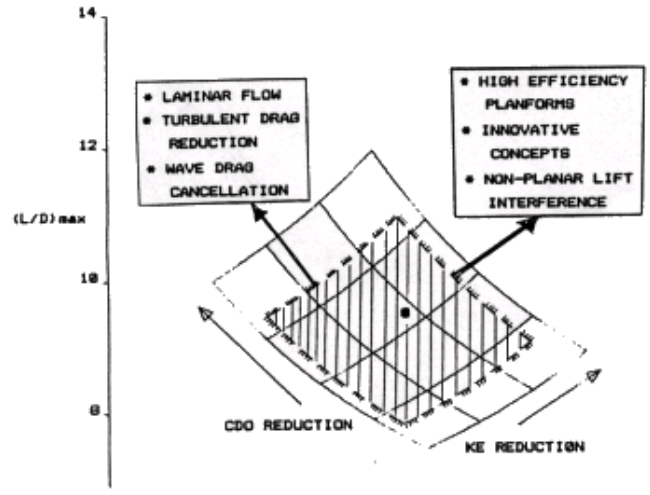

Figure 9 Potential (L/D)max Improvements - Technology Development

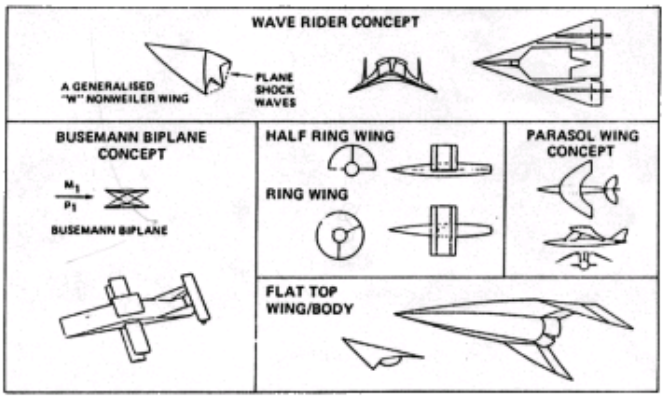

Figure 10 Hypersonic Favorable Interference Concepts

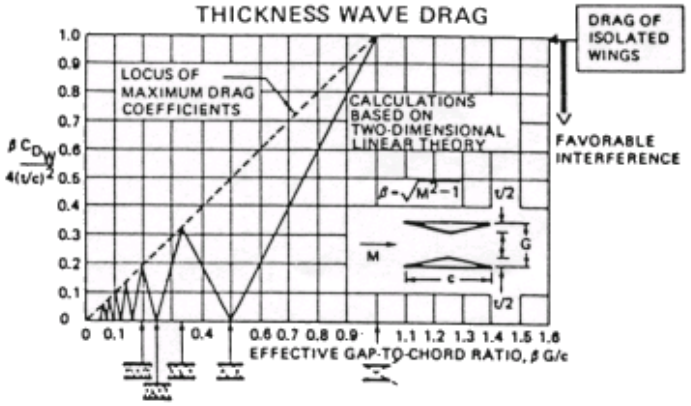

Figure 11 Busemann Biplane Thickness Wave Drag

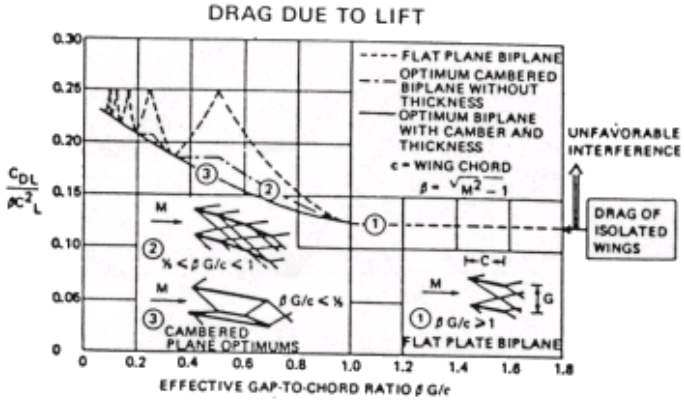

Figure 12 Busemann Biplane Drag Due to Lift

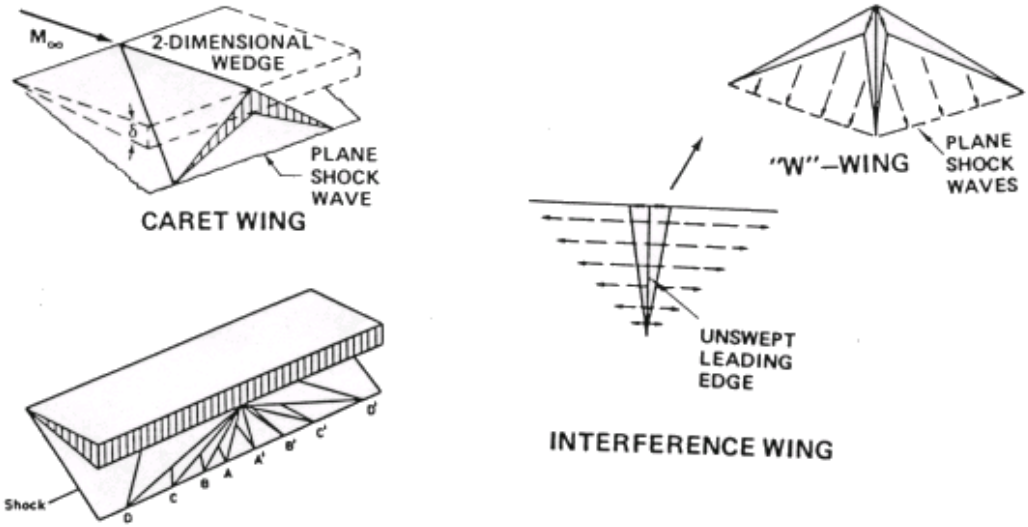

Figure 13 Caret and Nonweiler Wing Aerodynamics

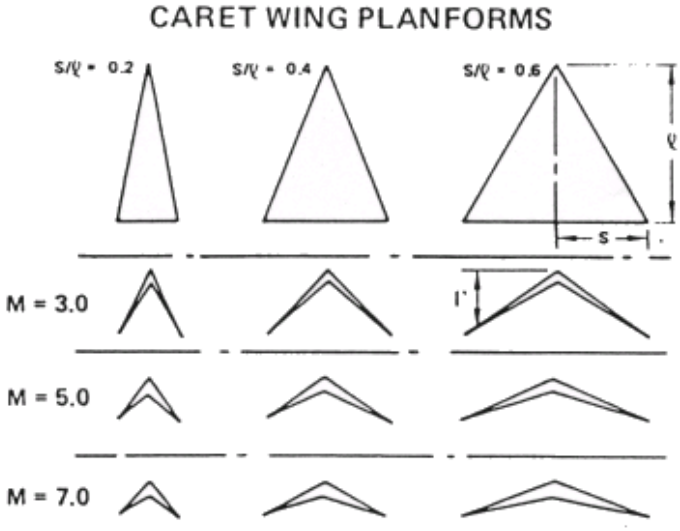

Figure 14 Caret Wing Planforms

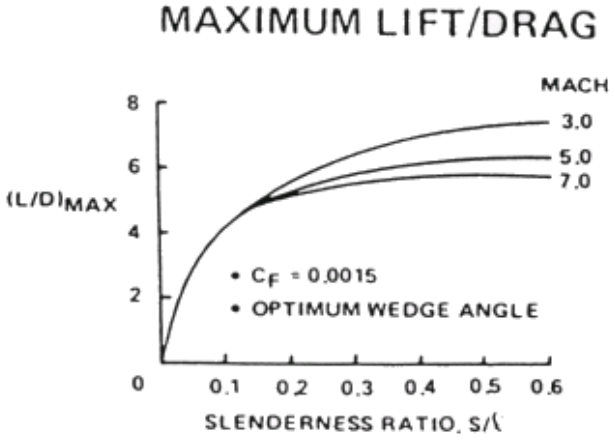

Figure 15 Caret Wing Maximum Lift/Drag Ratios

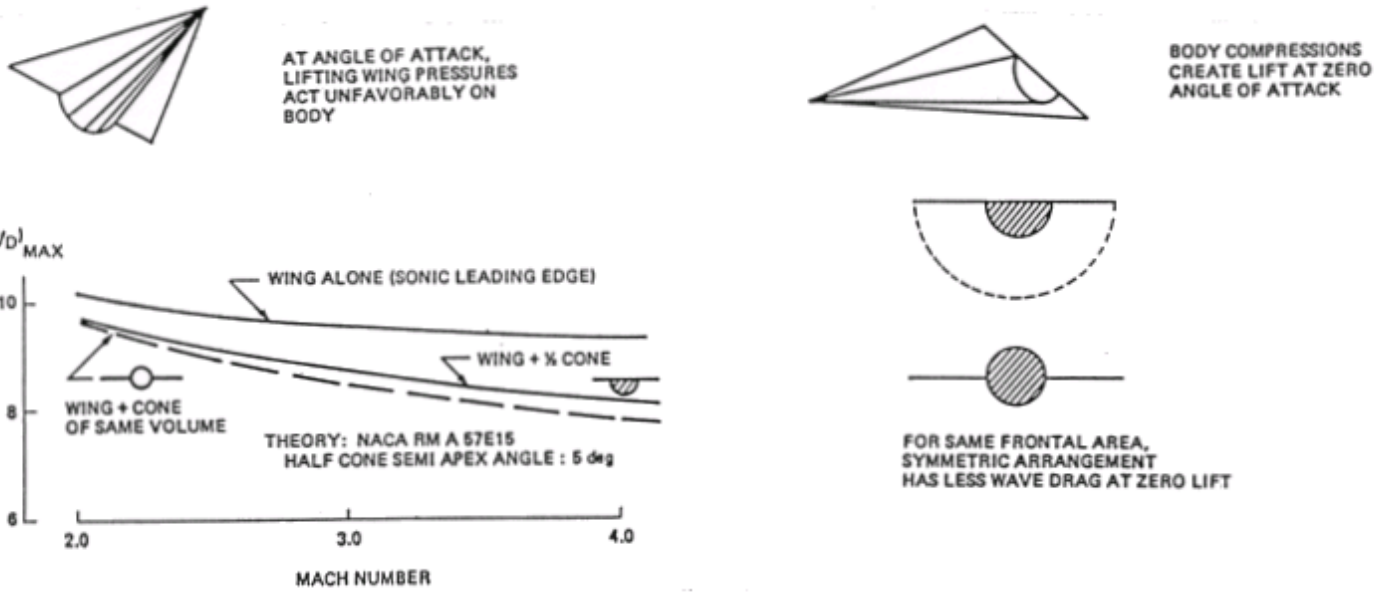

Figure 16 Flat-Top Wing/Body Aerodynamics

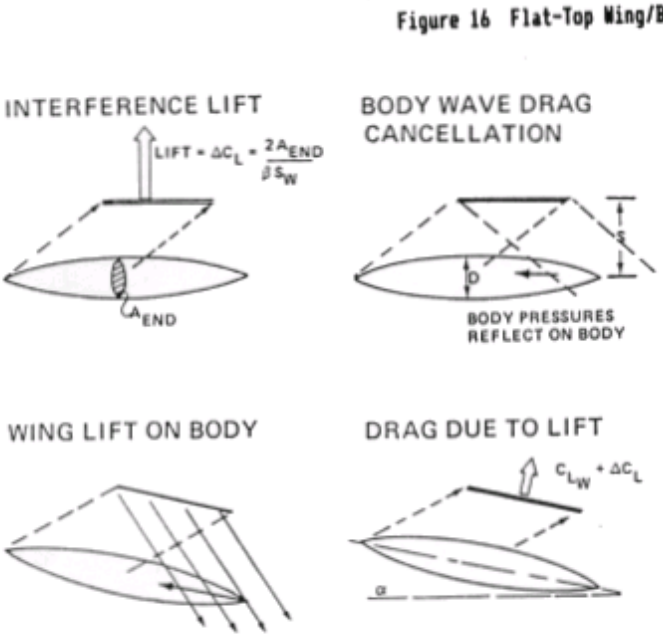

Figure 17 Parasol Wing Aerodynamics

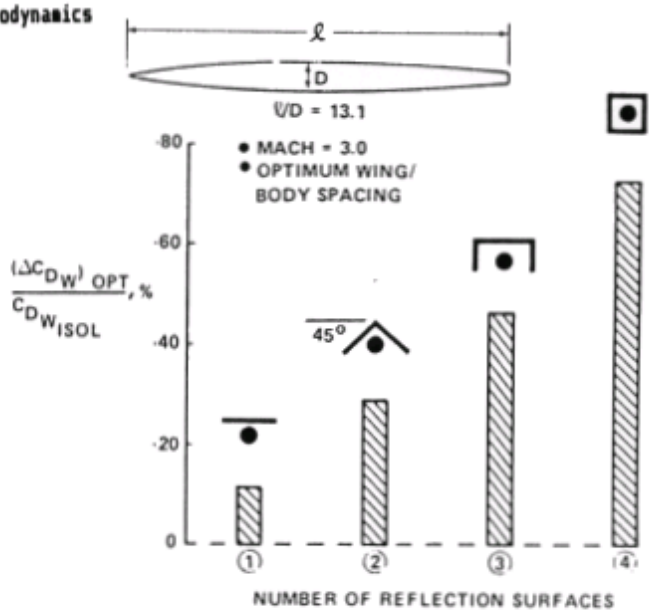

Figure 18 Ring-Wing and Parasol-Wing Wave Drag Cancellation

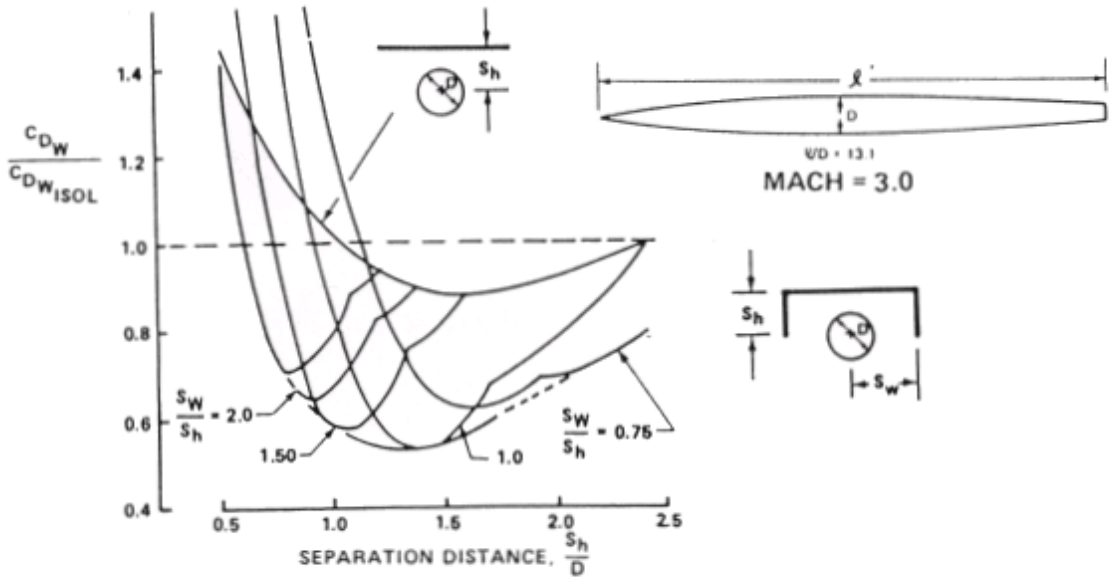

Figure 19 Rectangular Parasol-Wing Wave Drag Cancellation

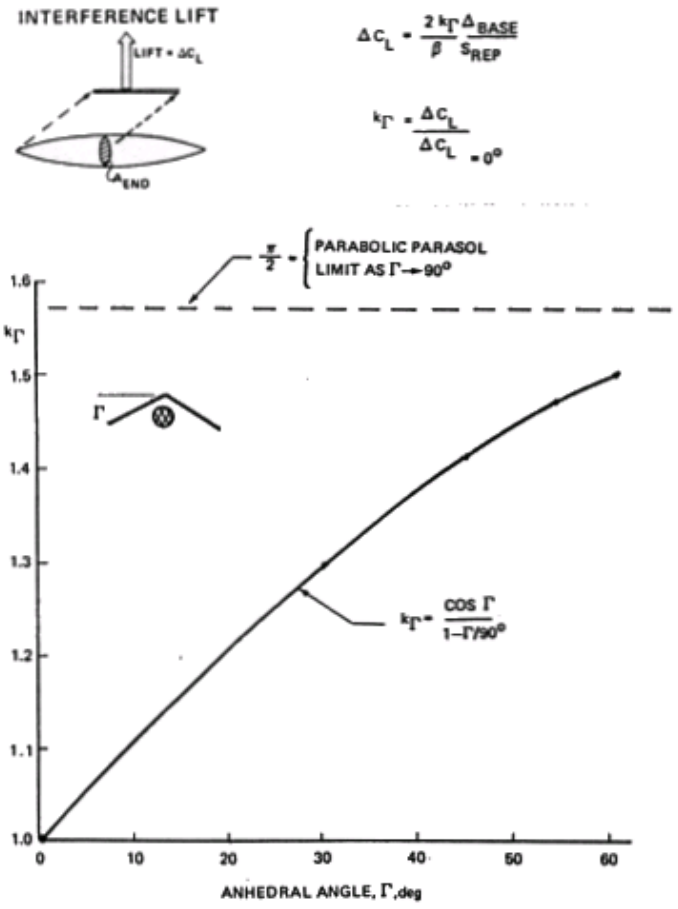

Figure 20 Effect of Anhederal Angle on Parasol-Wing Interference Lift

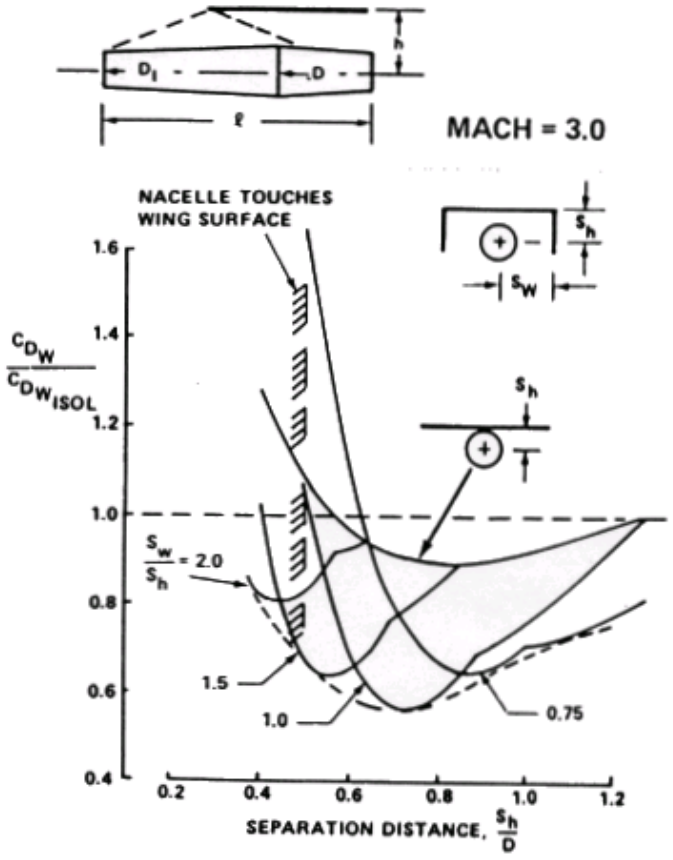

Figure 21 Nacelle Wave Drag Cancellation

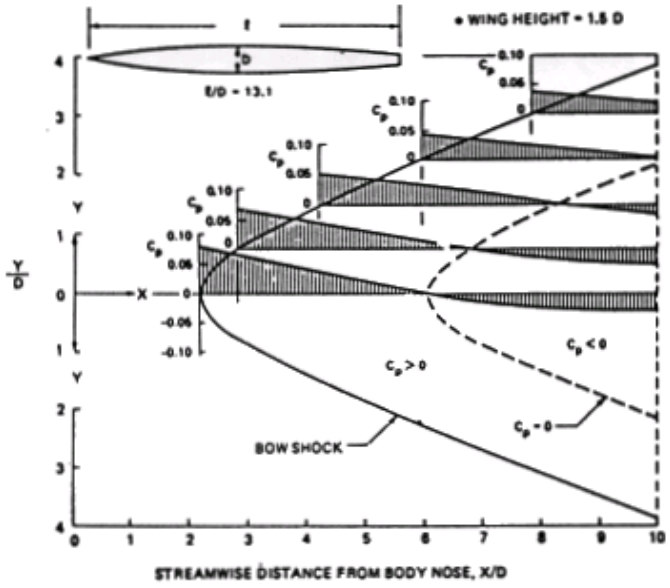

Figure 22 Interference Pressure Distribution - Fuselage

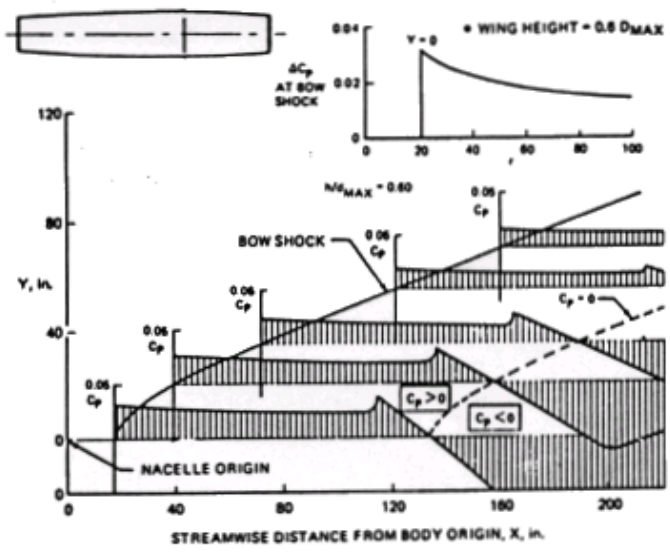

Figure 23 Interference Pressure Distribution - Engine Nacelle

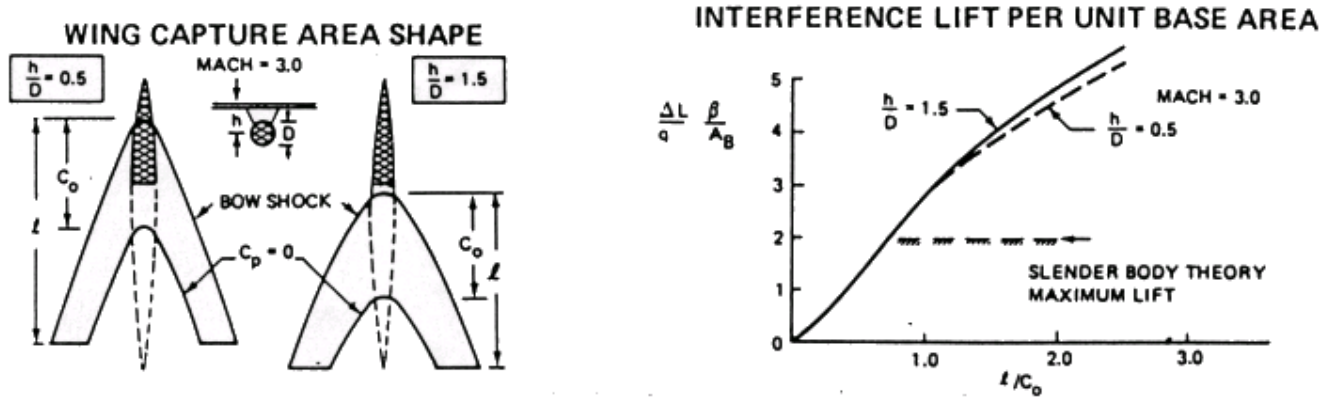

Figure 24 Effect of Planform Tailoring on Interference Lift

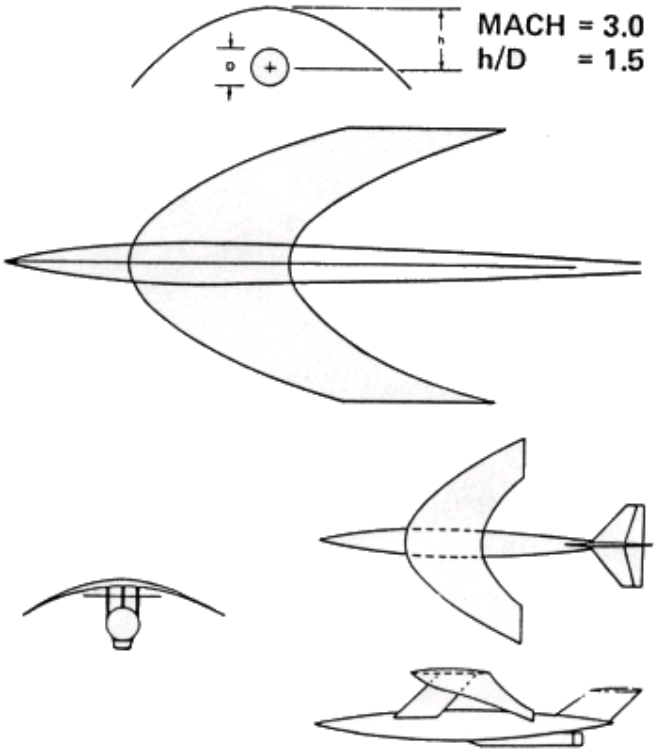

Figure 25 Body Parasol-Wing Configuration Features

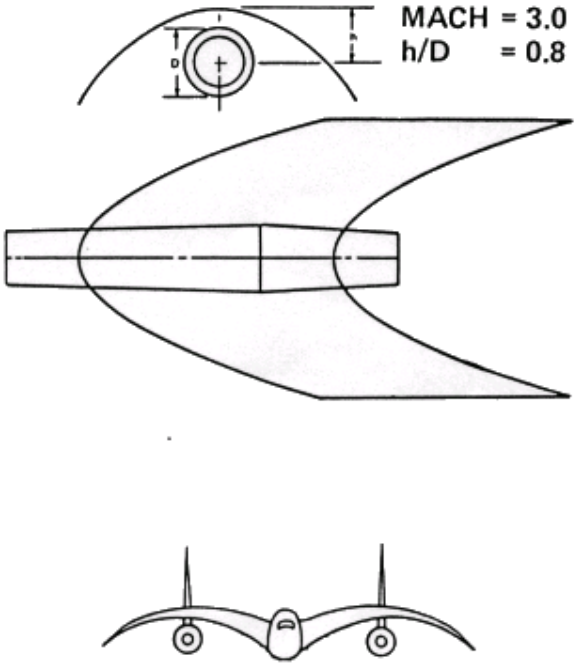

Figure 26 Nacelle Parasol-Wing Configuration Features

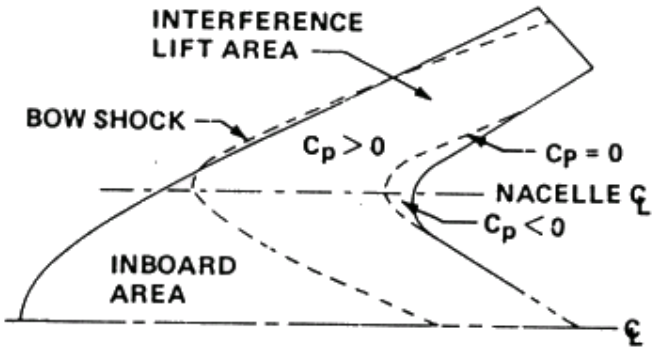

Figure 27 Double Parasol-Wing Planform Development

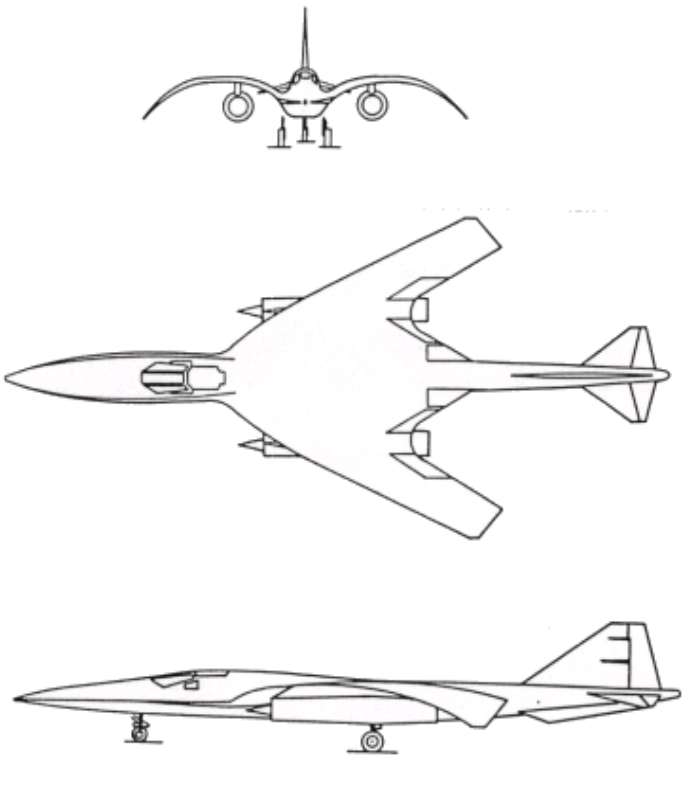

Figure 28 Double Parasol-Wing Configuration Definition

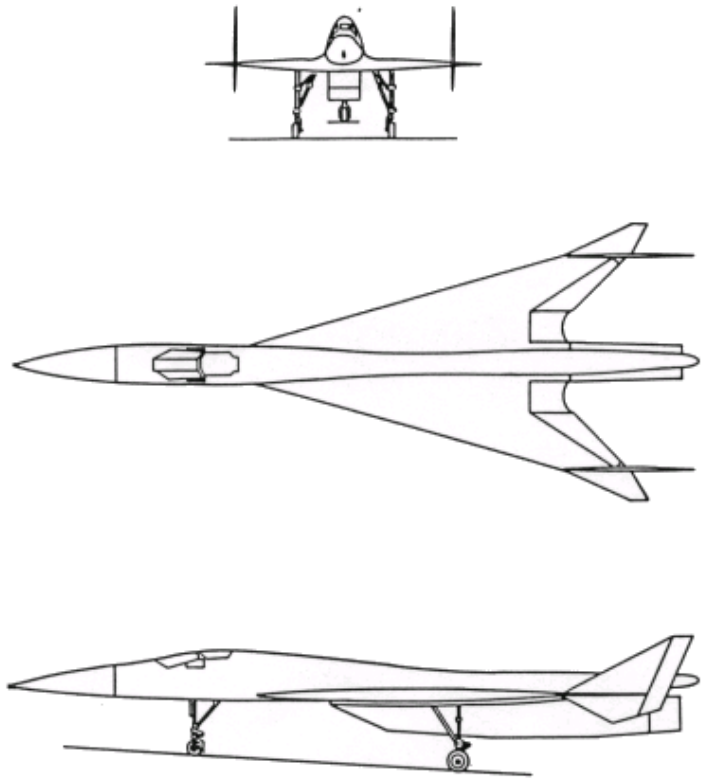

Figure 29 Reference Conventional Baseline Configuration

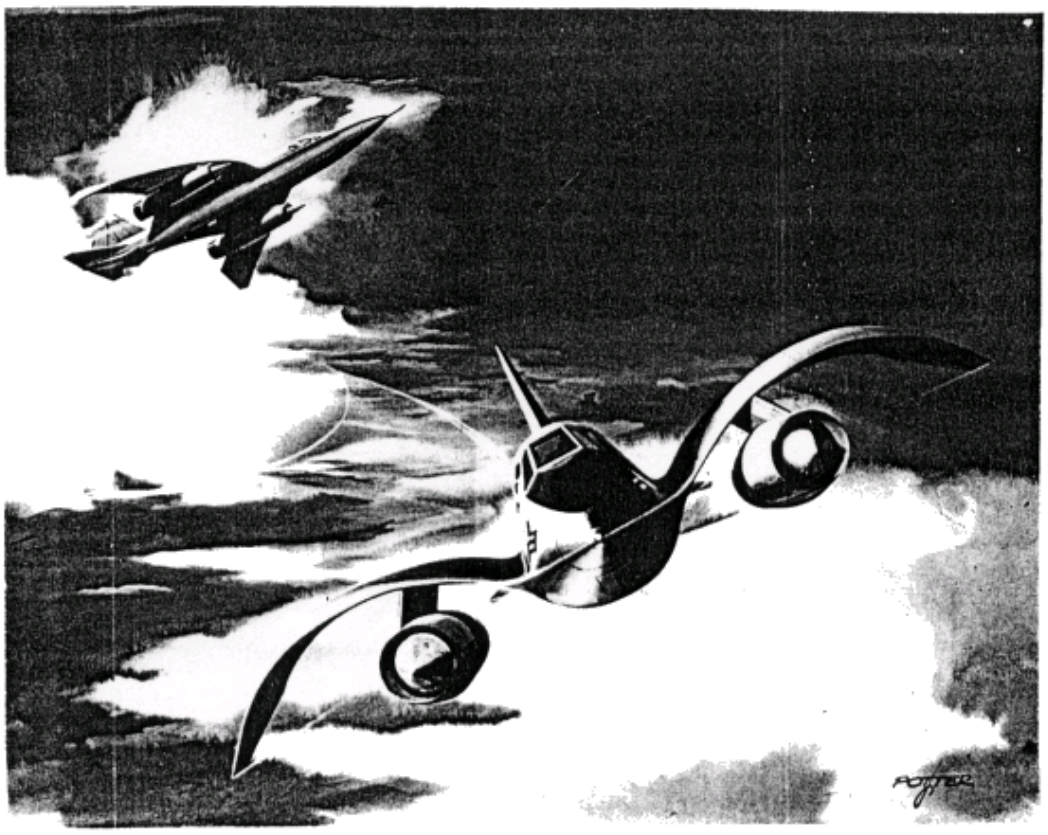

Figure 30 Double Parasol-Wing Configuration

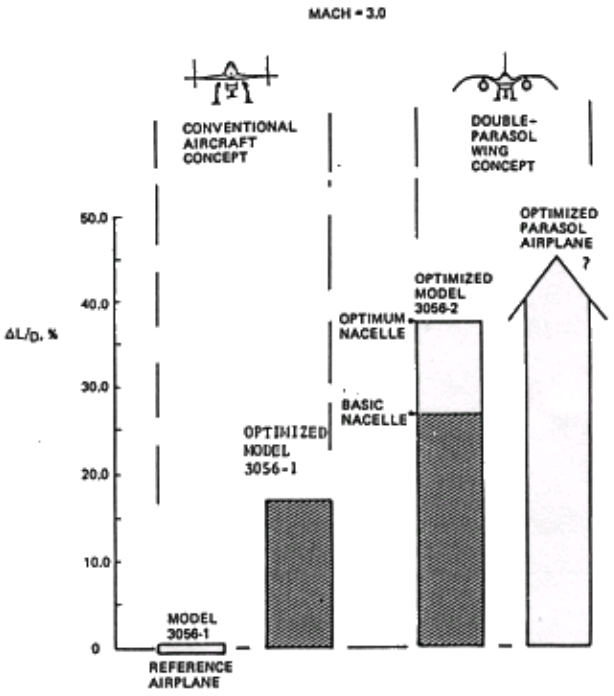

Figure 31 Double Parasol-Wing (L/D)max Improvement

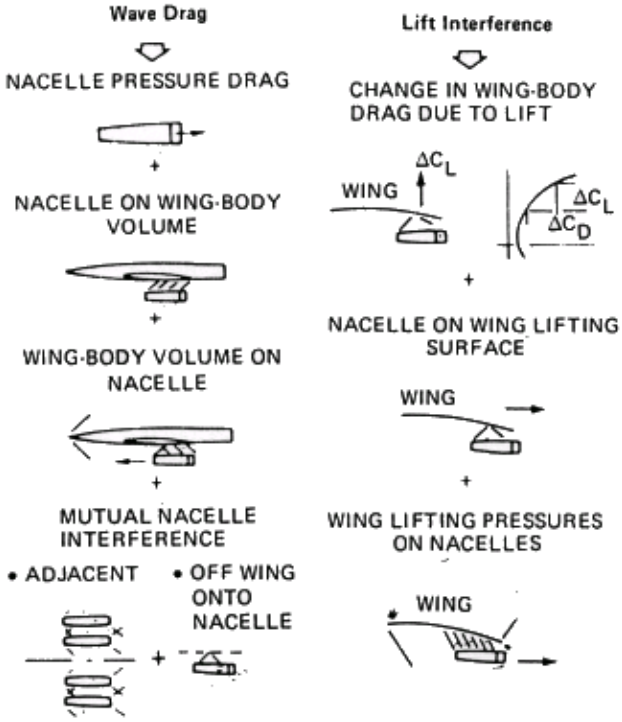

Figure 32 Nacelle Installed Drag Components

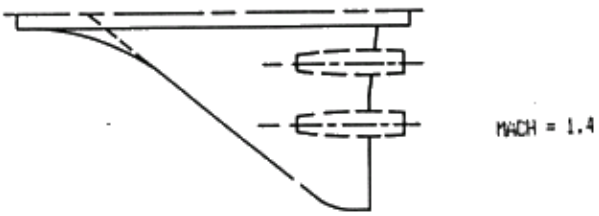

MACH = 1.4

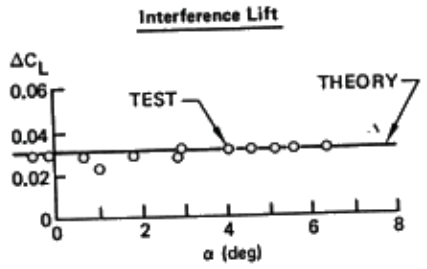

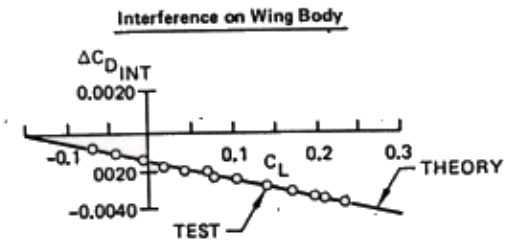

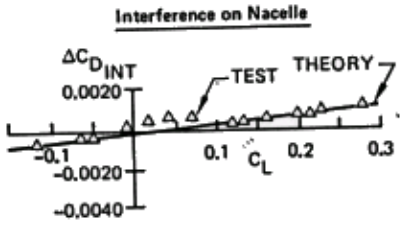

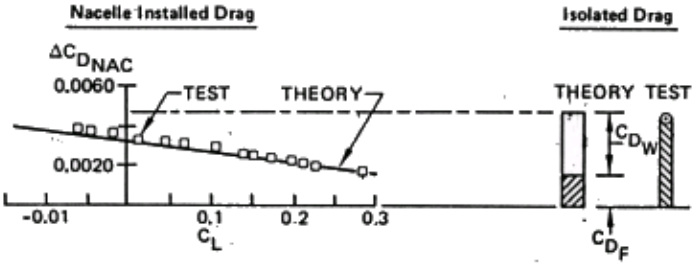

Figure 33 Installed Nacelle Drag -- Aft Location

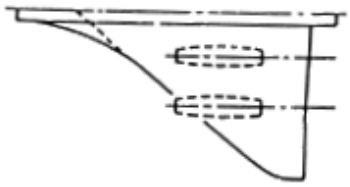

MACH = 1.4

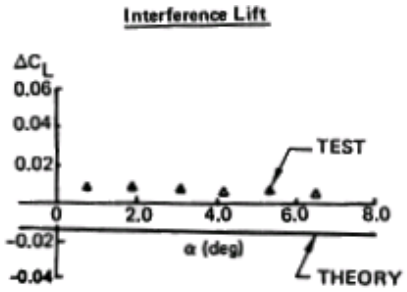

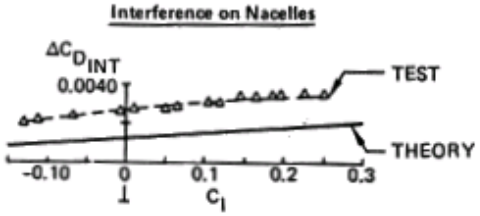

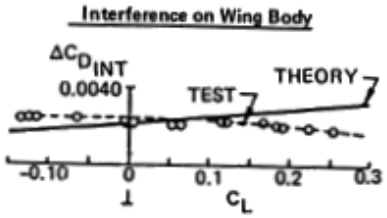

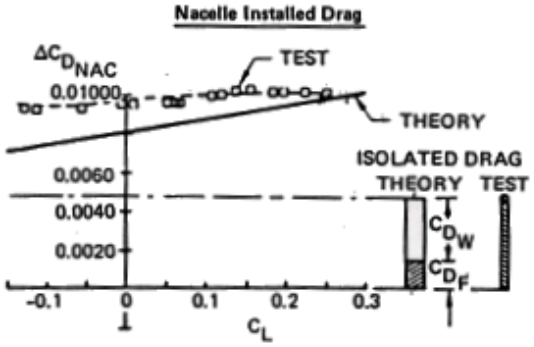

Figure 34 Installed Nacelle Drag - Forward Location

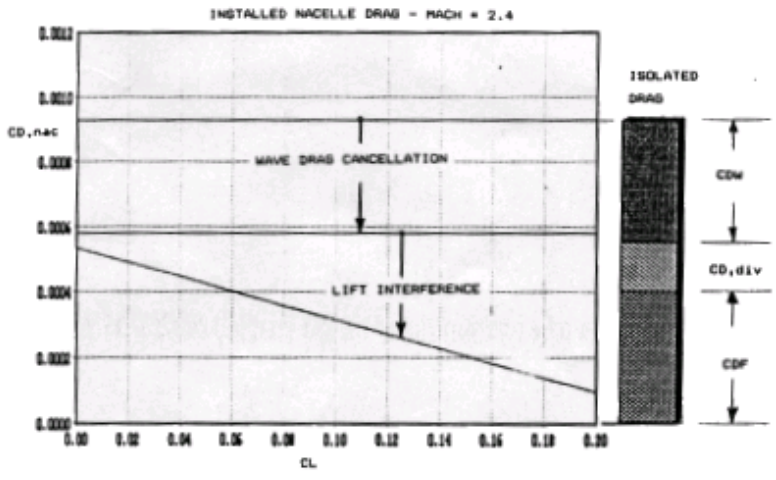

Figure 35 HSCT Optimized Nacelle Drag Components

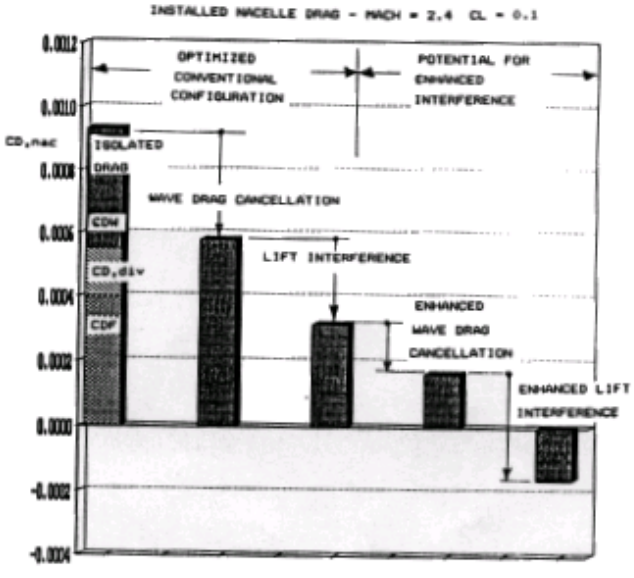

Figure 36 Potential Reductions in Nacelle Installed Drag